



Transfer of Melt Between Microscopic Pores and Macroscopic Veins in Migmatites

A. Simakin and C. Talbot

Hans Ramberg Tectonic Laboratory, Department of Earth Sciences, University of Uppsala, Villavagen 16, SE-752 36 Uppsala, Sweden

Received 14 June 2000; accepted 15 November 2000

Abstract. A new model is proposed to numerically simulate transfer of melt between microscopic pores and macroscopic veins in a deforming porous matrix. Matrix rheology is assumed to be visco-elastic. Darcy flow of porous melt through the matrix is calculated in accord with the theory of poroelasticity. Veins of melt are described separately. The model is realized using a code for a 2-D rectangle that is deformed at a constant strain rate. We reproduce in 2-D the main analytical results derived by Sleep (1988) but add calculations concerning the flow and local compaction processes around veins with different inclinations to the maximum (compressive) deviatoric stress. Inclusions perpendicular to σ_1 tend to close while those parallel to σ_1 tend to grow. Surrounding regions either compact or dilate and inclined veins propagate parallel to σ_1 . The incremental porosity decreases exponentially with distance from the vein walls by a factor equal to the compaction length. Local redistribution of melt from microscopic pores to macroscopic veins strongly enhances melt segregation into the vein networks which can lead to bodies sufficiently massive to become buoyant. © 2001 Elsevier Science Ltd. All rights reserved

1. Introduction.

Melt can segregate in a porous matrix in the mantle (Ribe, 1985) and in granitic migmatites (Brown et al., 1995). The main physical mechanism responsible for melt segregation is usually assumed to be gravity driving low density melt upward from a denser solid matrix that compacts. Equations to model compaction with melt segregation have been proposed by Sleep (1974) and developed by McKenzie (1984) and Scott and Stevenson (1986). These equations assume a simple Newtonian viscous rheology for the solid matrix which is appropriate for the high PT conditions and slow deformations considered here. Different types of

solutions can couple the hyperbolic equations for phases transfer with the elliptic momentum equations. There is the simple boundary layer-type solution where melt is expelled by compacting from the partially melted layer only near the assumed lower solid impermeable base (McKenzie, 1984). There are also soliton-like solutions representing blobs enriched in melt traveling in space (Scott and Stevenson, 1986). A new instability has recently suggested by Khodakovskii et al. (1995) leads to the formation of closely spaced layers with high melt content. This instability is connected with the effects that nonlinear porosity has on the matrix viscosity which can decrease abruptly by 2-6 orders of magnitude at a threshold value of about 5 vol%. If initial conditions lead to this threshold vol.% the melt is strongly concentrated in the train of rising melt-enriched layers. In principle, this mechanism could lead to the formation of layered structures which includes migmatites.

Another force that can segregate melt within a solid porous matrix is regional deformation due to a large scale tectonic movement. Segregation can result from compression along an initial plane layering decreasing the pressure of the melt distributed in the porosity of layers with the smaller matrix viscosity. Increasing the melt content (porosity) leads to a decrease in the viscosity of the matrix so that any small plane inhomogeneities in the porosity are unstable and develop into layers enriched in melt as noted by Stevenson (1989). Brown et al. (1995) explained migmatite formation in a similar manner. However, they assume extension along the initial plane layering and that melt segregates into the stiffer layers so that the viscosity equilibrates and further melt redistribution ceases.

Another mechanism for melt redistribution is the tapping of partial melt by melt-filled veins of appropriate orientation, as pointed out by Sleep (1988). He investigated analytically the pressure distribution around inclusion elongate parallel to the direction of compression. He showed that the pressure inside an inclusion is lower than in the surrounding viscous matrix and that this leads to melt migrating into veins as the vein walls compact. He

Correspondence to: A. Simakin.

E-Mail: simakin@iem.ac.ru; FAX: 007(096)5246205

developed equations describing some simple examples of this process. However, unlike the mechanism of gravitational compaction, this idea has not been developed further. To solve this problem, we use numerical solutions that describe the influence of geometry and other factors on crack (or vein) growth.

Here we slightly modify the equations governing the flow of partial melt around inclusions in a deformable 2D rectangle. We replace a viscous rheology for the matrix by a viscoelastic rheology. A viscoelastic rheology is appropriate for modeling tectonic processes in the crust where elastic rupture is possible (Rubin, 1993). Viscoelasticity is usually combined with a plastic rheology to take account of the formation of the shear zones or faults, (e.g., (Ord and Oliver, 1997)). We also directly apply poroelasticity theory (Detournay and Chen, 1993) to define the response of partial melt pressure on the volumetric strain. Our Numerical solution describes the deformation of a porous matrix and the consequent flow of melt from the matrix into veins which have different orientations relative to the axis of compressive deviatoric stress. We suggest that deformation can lead to differentiation of viscous granitic melts into medium scale veins that can lead to the generation of dykes or sills sufficiently voluminous to rise further in the crust by buoyancy.

2. Model equations

Simple viscous rheology is generally assumed to model the compaction of solid porous matrix (McKenzie, 1984; Sleep, 1988; Khodakovskii et al., 1995). However, deformations of solid matrix are also often described as elastic (reversible) in geomechanics (e.g. in considering the hydrofracturing of porous rock by overpressured fluid in a well by Boone and Ingraffea (1990)). Here we study the movement of melt through a macroscopic (vein) and microscopic (intergranular) paths in a partially molten viscoelastic rocks at high pressure and temperature. The immediate response of the porous matrix to the deformation is elastic so that poroelasticity theory can be applied (Detournay and Chen, 1993). The theory of poroelasticity was developed for composite materials consisting of a solid matrix with liquid filled pores and is based on phenomenological and micromechanical considerations. Effective stress (σ_e) is defined as the sum of the total stress (σ_{ij}) and pressure of the internal fluid:

$$\sigma_{e,ij} = \sigma_{ij} + \alpha P_i \delta_{ij} \quad (1)$$

where α is a Biot coefficient that varies from about 0.1 to 1 for a matrix with very low porosity to a porosity of 0.2-0.35. The effective strain in the elastic case is determined by the deviatoric and symmetric components of the strain tensor

$$\sigma_{e,ij} = \frac{2\mu\nu}{1-2\nu} e_{kk} \delta_{ij} + 2\mu e_{ij} \quad (2)$$

Melt pressure P_i is defined through variation of partial melt volume and incremental volumetric strain of the porous matrix as a full time derivative (in the moving matrix)

$$\dot{P}_i = M(\dot{\zeta} - \alpha \dot{e}_{kk}) \quad (3)$$

where ζ is liquid volume content. Poroelasticity constants are defined through the elastic properties of drained ($P_i=0$) and undrained ($d\zeta/dt=0$) matrix

$$\alpha = 1 - \frac{K}{K_u}, \quad M = \frac{K_u - K}{\alpha^2} = \frac{BK_u}{\alpha} \quad (4)$$

where K_u is the undrained bulk modulus. Skempton's coefficient B varies in the range 0.65-0.95. The total stress satisfies the equation of mechanical equilibrium:

$$\sigma_{ij,i} + f_i = 0 \quad (5)$$

where f is the body force, generally the gravitational force $f=(0,\rho g)$. Variations of liquid volume content are calculated in accordance with Darcy's law:

$$\dot{\zeta} = k \nabla^2 P_i + Q \quad (6)$$

where Q is a source term and the permeability is proportional to intrinsic permeability k_i and inversely proportional to melt viscosity (η_L) $k = k_i / \eta_L$.

The deviatoric stress σ_{ij}^d in the viscoelastic matrix will relax so that (see e.g. in (Poliakov et al., 1993)):

$$\dot{\sigma}_{ij}^d = 2\mu \dot{e}_{ij}^d - \frac{\sigma_{ij}^d}{\tau_1} \quad (7)$$

The relaxation time τ_1 is defined as a ratio of shear viscosity (η) and shear modulus (μ) $\tau_1 = \eta / \mu$. The first relaxation eliminates deviatoric stresses and provides possibility of large deformations.

We assume the second relaxation process that equates the mean solid stress and fluid pressure by local compression or dilation of pore space in the matrix

$$\dot{\sigma}_{e,ij} = 2K \dot{e}_{ij}^s \delta_{ij} - \frac{\sigma_{ij}^s + P_i}{\tau_2} \quad (8)$$

During slow deformations time derivatives of stress equal zero and equations (7) and (8) define viscous stresses (as e.g. in (McKenzie, 1984)) if second relaxation time equals ratio of volume viscosity to (in 2D) double the bulk modulus $\eta_v/2K$. Consequently, instead of constitutive equation (3) we will use equations (7,8)

In the following we consider processes on linear scales sufficiently small that the gravity term in Eq.(5) can be neglected. We also assume that the macroscopic veins are filled with melt. The shapes of veins deform as the matrix is strained. Pressure of the liquid inside i -th inclusion obeys the equation of state:

$$P_i = \Delta S_i(P_i) / S_{o,i} K_i \quad (9)$$

The stresses on the walls of all veins are in mechanical equilibrium (see e.g. in Zienkiewicz, 1989) so that

$$\sigma \cdot n(\Gamma_i) = P_i n(\Gamma_i), \quad (10)$$

where Γ_i is the vector of normal to the i -th vein boundary. The amount of melt in a vein changes due to Darcy flow

with filtration rate U_i . Such flow is driven by the difference in pressure between vein and melt in adjacent porous matrix such that

$$\frac{dS_{o,i}}{dt} = - \int_{\Gamma_i} n(\Gamma_i(r)) U_i(r) dr \quad (11)$$

Here we consider only a 2-D rectangle with one elliptical inclusion of variable orientation

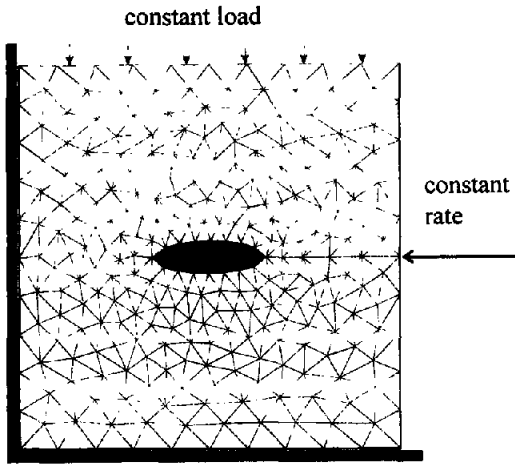


Fig.1. An example of the unstructured triangular grid used in calculations. Arrows demonstrate scheme of numerical experiments

The lower and left hand boundaries are symmetry boundaries with vertical and horizontal displacements equal to zero respectively (so the domain being considered can be translated downward and to the left -see Fig.1). The upper boundary is flexible with a constant load. Deformations are performed by moving the right boundary at a prescribed rate. On the whole this geometry resembles physical experiments for uniaxial shortening at high PT (e.g., Rutter and Neumann, 1995). The system of Equations (5,7,8,9,10,11) with the boundary conditions specified above was solved numerically by the FEM Galerkin method (Zienkiewicz,1989). The displacement field in incremental form is calculated on the deforming grid. The initial unstructured triangular grid (see Fig.1) of the size 2×2 in units L_0 that will be specified below was generated using a special program allowing the inclusion of several elliptical veins in the matrix.

We use bilinear triangular elements to solve the mechanical equilibrium equation in displacements while exploiting a time stepping scheme for relaxation as in (Poliakov et al., 1993). Increments of volumetric strain were used to solve Darcy's equation for pressure (Eq.(6)) on the triangular bilinear elements. The pressure field was then averaged on elements and used to calculate effective stress (Eq.(2)) and iteratively repeat solution of mechanic equilibrium (Eqns. (7,8)). Pressure in the vein is adjusted to melt flux (Eq. (11)) and deformations of the walls (Eq. (10)) using the Newton method on each iteration step.

3. Results

We use the following parameter values. Young modulus of the matrix E is taken as 50 GPa, bulk modulus of liquid K_L is taken as 100 GPa. The Poisson ratio of the matrix ν is 0.2. We take Skempton's coefficient $B=0.85$ and Biot constant $\alpha=0.3$. Shear and volume viscosities of the matrix are taken as 10^{17} Pa·s. We use a pressure scale $P_0=50$ MPa and a time scale $t_0=10^8$ sec. The length scale is arbitrary during calculations and is only important when defining dimensional values of the intrinsic permeability k_0 .

In our runs we assume correspondent dimensionless values of permeability (Eq.(6)) $k = k_0 P_0 t_0 / \eta_L L_0^2$ in the range 0.0007 - 0.012, where η_L is the viscosity of the granite melt, L_0 is the linear scale. Our case with $\eta_L = 10^5$ Pa·s and $L_0=1.0$ m will correspond to a intrinsic permeability (k_0) range of $1.3 \cdot 10^{-14}$ to $2.4 \cdot 10^{-13} \text{m}^2$. We shorten our rectangle with the material properties described above at strain rates $5 \cdot 10^{-10}$ - $2.5 \cdot 10^{-9} \text{s}^{-1}$. The results of calculations for veins with different orientation can be seen in Fig.2a-c displaying increments of porosity for the strain 0.025. Porosities increments have been calculated by integrating Eq.(6) in time.

All figures demonstrate areas of porosity that have increased or decreased in similar patterns. A horizontal melt-filled vein elongate in the direction of horizontal compression has an internal pressure lower than the adjoining porous matrix. As a result porous melt migrates into the inclusion as the walls of the inclusion compact. Although the vein propagates by cracking the matrix, its horizontal propagation is aided by matrix porosity increasing in narrow zones around both tips of the vein (Fig.2a). Melt pressure in the vertical vein (Fig.2b) is higher than in the adjoining matrix so melt is expelled from it forming diffusing halo (a surrounding region of increased porosity). Regions of compaction and dilation are almost equal in area around an inclusion inclined by 45° to compression axis (Fig.2c). However, asymmetry of these regions tends to redistribute the melt in the surrounding matrix so that the vein propagates horizontally.

Over a range of parameters tested we find the distribution of incremental porosity to occur in similar special patterns on absolute scales that increased as predicted by a simple solution considered by Sleep (1988). He demonstrates that in the contact with infinite planar inclusion the porous melt pressure, velocity, resulted incremental porosity vary as $f(t) \exp(-z/\delta_c)$, where z is distance from the inclusion surface and δ_c is compaction length equals

$$\delta_c^2 = \frac{k_0 (\eta_L + 2\eta)}{\eta_L} \quad (12)$$

Compaction length is a natural linear scale that arises in the compaction problem. Compaction in central cross-section perpendicular to the horizontal vein (Fig.2a) is well described in this way. Difference between compaction

length value from Eq.(12) and from approximation of porosity distribution from Fig. 2a along line crossing inclusion perpendicular to the long axis through the center is about 5% (theoretical value of δ_c equals 0.245 and numerical estimate is about 0.257).

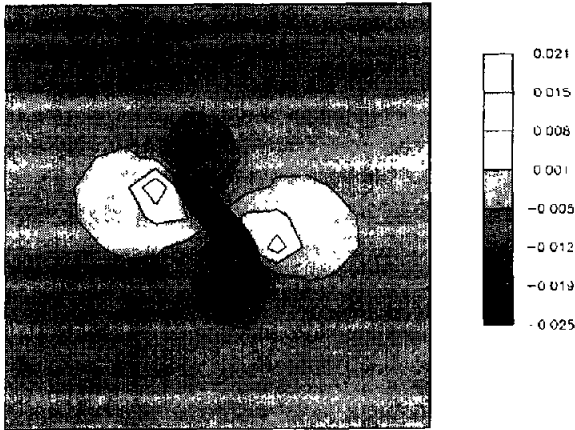


Fig.2. Incremental porosity after deformation in a shortened matrix Total strain 0.025, permeability $k = 4 \cdot 10^{-14} m^2$, $\alpha = 0.3$, Skempton's coefficient $B = 0.85$
a) around horizontal vein

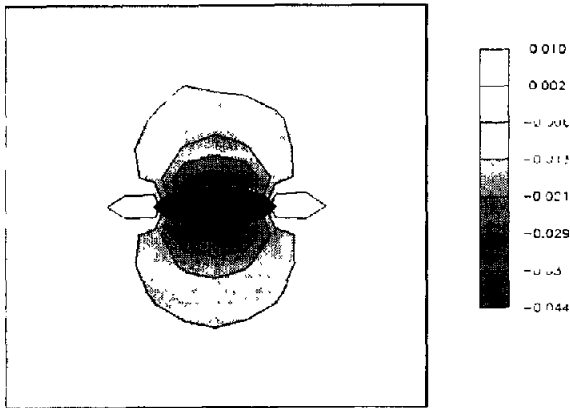


Fig.2. b) around tilted vein

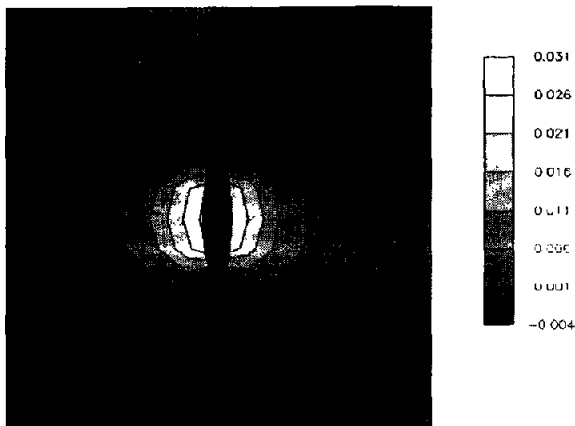


Fig.2. c) around vertical vein

Figure 3d shows dependence of integrated melt flux into (of) an inclusion normalized on the initial volume (surface in 2-D) of veins, total strain is 2.5 %. Quasi-steady state is reached in approximately 0.1 t_3 at the parameters assumed.

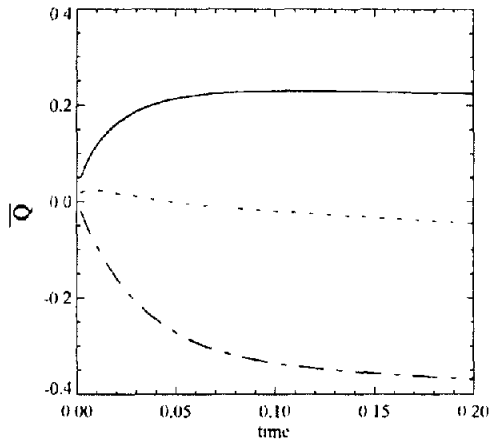


Fig.3. Time dependence of melt flux integrated by contour of vein (Eq (10)), where solid line indicates horizontal, dotted line inclined and dots-dashes vertical veins, time in 10^8 s. Parameters values correspond to those in Fig 2

Inclined by 45° inclusion rotates and gets more steep (approaching vertical with time) orientation that reflects on the variation of flux that is positive at the initial moment and becomes negative later. Flux from the vertical inclusion is larger than to the horizontal one.

4. Discussion

Our results confirm the conclusion reached by Sleep (1988): that melt is pumped into an inclusion parallel to the shortening direction. We can also add that veins with appropriate orientation can shrink or rotate as they tend to propagate in the direction of maximum compressive stress. Linear scale of the melt redistribution is defined by the compaction length (Eq.(12))

The value of the compaction length will be $5 \cdot 10^{-5} - 0.5$ m for the granites with volume and shear viscosities of solid matrix equal to 10^{17} Pa·s, melt viscosity equal to $10^3 - 10^6$ Pa·s and intrinsic permeability $k_0 = 10^{-13} - 10^{-16} m^2$. Even lower values of permeability are measured experimentally (down to $10^{-20} m^2$) in the natural rocks with porosity of several percents (Shmonov et al., 1995) depending on the rock texture. However, higher values (up to $4 \cdot 10^{-13} m^2$ for porosity 2%) are expected in partially melted rocks (Khodakovskii et al., 1995). We therefore anticipate that porous flow on the grain scale will constrain melt redistribution to the small scales observed in migmatites. Shear veins that also absorb melt (Collins and Sawyer, 1996) are beyond the scope of our model.

The alternative mechanism of gravity compaction with a strong nonlinear dependence of matrix viscosity on its porosity of Khodakovskii et al.(1995) can also be used to explain the formation of migmatites with horizontal layering. However, the vertical, inclined, or folded

syntectonic layering in many migmatites require another process. The tectonic pumping modeled here will facilitate segregation of partial melts into layered migmatites in rapidly deforming regions.

We anticipate that introducing the porosity dependent matrix viscosity and permeability would improve our model to the stage where it could explain the dark envelopes (mafic compaction zones) around so many veins of in-situ granite in many migmatites.

Acknowledgements Authors are grateful to N Sleep for his very useful discussion to and thanks V Trubitsyn and anonymous reviewer for their instructive suggestions. This study was funded by the Royal Academy of Science in Sweden

References

- Boone, T J and Ingraffea, A R, 1990 A numerical procedure for simulation of hydraulically-driven fracture propagation in poroelastic media *Intern. J. Numer. and Anal. Methods in Geomech.* 14: 27-47
- Brown, M., Averkina, Y., McLellan, E L., and Sawyer, E., 1995 Melt segregation in migmatites *J. Geophys. Res.* 100, 15 655-15 679
- Collins, W.J. and Sawyer, E W 1996 Pervasive granitoid magma transfer through the lower-middle crust during non-coaxial compressional deformations *Journ. Met. Geol.*, 14:565-579
- Detournay, E and Chen, A., 1993 Fundamentals of poroelasticity In J A Hudson (Editor). *Comprehensive rock engineering Pergamon Press V2 Analysis and design methods* pp 113-171
- Khodakovskii, G., Rabinowicz, M., Ceuleneer, G., and Trubitsyn, V P., 1995 Melt percolation in a partially molten mantle mush: Effect of a variable viscosity *Earth Planet. Sci. Letts.* 134:267-281
- McKenzie, D P., 1984 The generation and compaction of partially molten rock *J. Petrol.* 25:713-765
- Ord, A and Oliver, N H S., 1997 Mechanical controls on fluid flow during regional metamorphism: some numerical models *J. Metam. Geol.* 15 345-359
- Poliakov, A., Podladchikov, P C Y., and Laykhovskiy, V., 1993 An explicit inertial method for simulation of viscoelastic flow: An evaluation of elastic effects on diapiric flow in two- and three- layers models. In: D B Stone and S K Runcom (Editors), *Flow and Creep in Solar System: Observations, Modelling and Theory*. Kluwer Acad Publ, pp 175-195
- Ribe, N., 1985 The generation and composition of partial melts in the earth's mantle *Earth Planet. Sci. Letts.* 73 361-376
- Rubin, A., 1993 Dikes vs diapirs in viscoelastic rock *Earth Planet. Sci. Letts.* 117 653-670
- Rutter, E H and Neumann, D H., 1995 Experimental deformation of partially molten Westerly granite under fluid-absent conditions, with implications for extraction of granite magmas *J. Geophys. Res.* 100:15 697-15 715.
- Scott, D and Stevenson, D J., 1986 Magma ascent by porous flow *J. Geophys. Res.* 91: 9283-9296.
- Sleep, N H., 1974 Segregation of magma from a mostly crystalline mush *Geol. Soc. Am. Bull.* 85 1225-1232
- Sleep, N H., 1988 Tapping of melt by veins and dikes *J. Geophys. Res.* 93 10 255-10 272
- Stevenson, D J., 1989 Spontaneous small-scale melt segregation in partial melts undergoing deformation *Geophys. Res. Letts.* 16 1067-1070
- Shmonov, V M., Vitovtova, V V., and Zarubina I V., 1995 Permeability of rocks at elevated temperatures and pressures. In: K I Shmulovich, W D Yardley and G G Gonchar (Editors) *Fluids in crust: Equilibrium and Transport properties*. Chapman & Hall London pp 285-312
- Zienkiewicz O C and Morgan K., 1986 *Finite elements and approximation*. Mir, Moscow, pp 318 (Russian edition)

Appendix A

Mechanical variables

- σ - stress tensor
- ϵ - strain tensor
- P_l - pressure of melt in the vein
- U_l - vector of melt velocity
- Γ - curvature of vein boundary

Poroelasticity constants

- K_s - bulk modulus of solid material
- K_u - bulk modulus of matrix filled with liquid
- K - bulk modulus of drained porous matrix
- B - Skempton coefficient
- α - Biot constant
- M - Biot modulus

Other material properties

- E - Young modulus
- k - permeability
- μ - shear modulus
- ν - Poisson coefficient
- η - viscosity
- ζ - volume content of liquid